Metabolomics (2019) 15:109
https://doi.org/10.1007/s11306-019-1571-9

ORIGINAL ARTICLE

Beyond the antibodies: serum metabolomic profiling of myasthenia gravis

Derrick Blackmore[1] · Zaeem Siddiqi[1] · Liang Li[2] · Nan Wang[2] · Walter Maksymowych[3]

Received: 8 January 2019 / Accepted: 23 July 2019 / Published online: 1 August 2019

Abstract

Introduction Myasthenia gravis (MG) is a chronic, potentially debilitating autoimmune disease characterized by weakness and rapid fatigue of the voluntary muscles that worsens on exertion. Left untreated, MG symptoms may cause significant morbidity or even death. To date, no robust biological marker is available to follow the course of the disease. Therefore, new diagnostic approaches and biological markers are essential not only for improved diagnosis of the disease but for improved outcomes.

Objectives The present study applied a two-control, multi-label metabolomics profiling approach as a potential strategy for the identification of biomarkers unique to myasthenia gravis (MG).

Methods Metabolic analyses using acid- and dansyl-labelled serum from seropositive MG (n = 46), rheumatoid arthritis (RA) (n = 23) and healthy controls (HC) (n = 49) were performed on samples from adult patients presenting to the University of Alberta Hospital neuromuscular and rheumatology clinics. Comparisons between patients with MG vs. HC, and RA vs. HC were made using univariate and multivariate statistics.

Results Serum biomarker patterns were statistically significantly different between groups. Principal component analysis (PCA) and partial least squares discriminant analysis (PLS-DA) models exhibited considerable distinction between all groups. Metabolites were then filtered to remove peak pairs common to both disease cohorts. Combined metabolite panels revealed clear separation between MG and HC for both library-matched (AUROC: 0.92 ± 0.03) and highest AUC patients (AUROC: 0.94 ± 0.05).

Conclusion In patients presenting to the clinic with seropositive MG, metabolomic profiling is capable of distinguishing patients with disease from those without. These results provide an important first step towards a potential biomarker for improving MG identification.

Keywords Metabolomics · Serum · Autoimmune · Myasthenia gravis · Rheumatoid arthritis · Immunometabolomics · Neuromuscular disease

✉ Derrick Blackmore
dblackmo@ualberta.ca

Zaeem Siddiqi
zsiddiqi@ualberta.ca

Liang Li
liang.li@ualberta.ca

Nan Wang
nanw@ualberta.ca

Walter Maksymowych
walter.maksymowych@ualberta.ca

[1] Division of Neurology, University of Alberta, 7th floor, Clinical Sciences Building, 11350 - 83 Ave NW, Edmonton, AB T6G 2G, Canada

[2] Department of Chemistry, University of Alberta, Chemistry Centre Room W3-39C, Edmonton, AB T6G 2G2, Canada

[3] 568A Heritage Medical Research Centre, University of Alberta, Edmonton, AB T6G 2S2, Canada

1 Introduction

Myasthenia gravis (MG) is a chronic autoimmune neuromuscular junction disorder characterized by the breakdown of normal communication between nerves and muscles, resulting in fluctuating weakness of the voluntary muscle groups. Rapid, accurate diagnosis of MG presents a challenge, particularly in the emergency room setting. Patients may not present with the typical symptoms, frequently mimicking other neurological conditions, such as stroke, or Gullain Barré Syndrome that can also produce facial and limb weakness like that seen in MG.

Biomarkers confirming MG are few and primarily diagnostic in nature. To date, no single biomarker has demonstrated reliable predictive power in MG. Serum antibodies are limited to diagnosis and differentiation of MG subtypes. In limited cases, such as muscle specific kinase (MuSK) antibodies, the response to therapy can be anticipated as refractory; this rarely informs the care of the patient, however. Electrophysiological studies are often used for the diagnosis of MG; these may be limited by factors related to accuracy, reproducibility and availability. Indeed, significant practice variation in the diagnosis of MG has been recognized, further illustrating the need for novel methods of diagnosis.

In the present study we aim to evaluate the potential of a multiplexed, dual- control metabolomics-based approach to aid the diagnosis and management of MG. Metabolites represent the intermediary and final products of the metabolic pathways within an organism; therefore, it is possible to achieve unique insight by studying these compounds under any given physiological condition. In addition, profiling of the extended spectrum of chemically-labelled species could provide an expanded understanding of the overall immune response. In pilot studies, other groups have explored the feasibility of a metabolomic approach for differentiating MG patients from healthy controls. To the best of our knowledge, however, no metabolomic study of autoimmune disease has attempted to remove the confounding effects of common pathophysiology, such as generalized immune responses. The aim of the present study is to apply a novel humoral-disease control approach to accurately identify unique metabolomic serum biomarkers, which distinguish patients presenting with seropositive MG from a reference autoimmune disease i.e. Rheumatoid arthritis (RA) and healthy controls.

2 Methods

2.1 Clinical characteristics of study subjects

This study was conducted in accordance with the Declaration of Helsinki ethical principles for medical research involving human subjects and received ethics approval from the University of Alberta Research Ethics Board and operational approvals from Alberta Health Services. Each study patient provided his/her informed consent for the study.

We prospectively enrolled 50 seropositive MG, and 50 seropositive RA patients, and 50 healthy controls (HC). MG and RA serostatus was confirmed with antibody testing for either anti-AChR (MG) or rheumatoid factor (RA). For the purposes of this study, ocular and generalized MG subtypes were considered phenotypically identical and serum sample were collected from both. RA patients were diagnosed in accordance with the American Rheumatology Association 1987 criteria (Hutchinson 1999). To exclude the confounds of race, only Caucasian patients were included in this study. There were no smokers and no statistically significant differences between all groups from time of last meal or BMI.

Clinical patients and healthy controls were enrolled in a prospective observational trial to obtain serum. MG and HC were collected within the same clinic. RA samples were collected in multiple clinics. Study subjects were age and gender matched, within the limitations of opportunistic sampling in the clinical setting. Further, patients had no history of any other autoimmune disease or thymoma. Finally, due to the nature of recruitment, patients were not required to fast.

24 ml blood samples were drawn from the anticubital vein using a 21 G needle and vacutainer® red top no additive tubes (Becton Dickenson Ref: 366408). Collected samples were allowed to clot for 30 min, at which time serum was drawn using a 0.2 um syringe filter and dispensed into a sterile labelled 15 ml centrifuge tube (Corning part # 431224). The blood samples were centrifuged at 2200×*g* for 10 min at 4 °C within 45 min and the serum was immediately frozen on dry ice. Collected samples were stored at − 80 °C until further use.

2.2 Metabolite extraction and labelling

2.2.1 Dansylation labelling

In brief, frozen serum samples were thawed on ice, vortexed to dissolve precipitates and then centrifuged at 14,000 rpm for 10 min. 25 µL supernatant was transferred into an Eppendorf tube and was mixed with 75 µL cold methanol. The mixture was then incubated on ice for 15 min to precipitate any proteins. Next, the mixture was centrifuged at 14,000 rpm for 15 min. 75 µL supernatant was taken and dried using a SpeedVac. The sample was reconstituted in 50 µL 1:1(v:v) Water/ACN solution. An aliquot of 25 µL serum solution was then mixed with 25 µL of 250 mM sodium carbonate/sodium. This bicarbonate buffer was further added into the sample to make a basic environment for the dansylation reaction. The solution was vortexed, spun down, and mixed with 25 µL of freshly prepared ^{12}C-dansyl chloride

solution (18 mg/mL) (for light labelling) or ^{13}C-dansyl chloride solution (18 mg/mL) (for heavy labelling). After 45 min incubation at 40 °C, 5 µL of 250 mM NaOH was added to the reaction mixture to quench the excess dansyl chloride. The solution was then incubated at 40 °C for another 10 min. Finally, 25 µL formic acid (425 mM) in 1:1(v:v) ACN/H2O was added to acidify the solution.

2.2.2 DmPA (dimethylaminophenacyl) labelling

For DmPA labelling after protein precipitation, an aliquot of 20 µL reconstituted serum sample (described above) was mixed with 20 µL water and 5 µL 6 M HCl solution, then followed by adding 5 µL of saturated NaCl solution. The vial was vortexed, then spun down and the sample was extracted using 150 µL ethyl acetate. Each vial was further vortexed for 30 s and then centrifuged at 8000 rpm for 5 min. The organic phase was transferred into another centrifuge vial with a screw cap and the pH was adjusted to 8 by adding 20 µL TEA solution (20 mg/mL in acetonitrile). Afterwards, the sample was dried down by using SpeedVac and then reconstituted in 30 µL TEA solution (10 mg/mL in acetonitrile). A solution of either ^{12}C-DmPA or ^{13}C-DmPA (10 mg/mL in acetonitrile) was added into the vial. The vial was again vortexed and spun down. Finally, the vial was incubated in an oven at 85 °C for 55 min.

2.2.3 LC-UV quantification

Sample amount was normalized using a protocol previously described (Zhao et al. 2016) based on LC-UV measurement of the total concentration of dansyl or DmPA labelled metabolites in a sample. A Waters ACQUITY UPLC system with a photodiode array (PDA) detector was used. 4 µL (dansyl-labelled) or 1 µL (DmPA-labelled) of each labelled serum sample was injected onto a Phenomenex Kinetex C18 column (50 mm × 2.1 mm, 1.7 µm particle size, 100 Å pore size) for a fast-step gradient run. Solvent A was 0.1% formic acid/5% ACN/water(v/v/v), and solvent B was 0.1% formic acid/ACN((v/v). The step gradient started with 0% B for 1 min and was increased to 95% within 0.01 min and held at 95% B for 1 min to ensure complete elution of all labelled metabolites. The flow rate was set at 0.45 mL/min. The total peak area of the labelled metabolites was measured at 338 nm and integrated using the Empower software (6.00.2154.003). Based on the quantification results, the ^{12}C- and ^{13}C -labelled samples were then mixed in equal amounts.

2.2.4 LC-QTOF-MS

Labelled serum samples were analyzed using a Bruker HD Impact quadrupole time-of-flight (QTOF) mass spectrometer (Billerica, MA, U.S.A.) with ESI linked to an Agilent 1100 series HPLC system (Palo Alto, CA, U.S.A.) along with an Agilent eclipse plus C18 column (100 mm × 2.1 mm, 1.8 µm particle size, 95 A pore size). LC Solvent A was 0.1% formic acid/5% ACN/water(v/v/v), and solvent B was 0.1% formic acid/ACN((v/v). The gradient elution profile was as follows: t = 0 min, 20% B; t = 3.5 min, 35% B; t = 18.0 min, 65% B; t = 24.0 min, 99% B; t = 28.0 min, 99% B. After each injection, the column was re-equilibrated with the initial mobile phase conditions for 15 min. The flow rate was set at 180 µL/min. Sample loading amount was optimized (data not included) and the same amount of each mixed sample was injected into the LC-MS system according to the LC-UV quantification result. The flow was loaded to the electrospray ionization (ESI) source of a Bruker maXis impact high-resolution quadrupole time-of-flight (Q-TOF) mass spectrometer (Bruker, Billerica, MA). All MS spectra were obtained in the positive ion mode.

2.2.5 Data processing

After LC-QTOF-MS analysis, entire peak lists were exported from Bruker Data Analysis software with a signal-to-noise threshold of 3. An in-house IsoMS software was used for peak-pair picking, peak-pair filtering, and peak-pair intensity ratio calculations (Zhou et al. 2014). The program eliminates false-positive peaks such as dimers and common adducts. A zero-fill program developed in-house was used afterwards to fill in missing values in the CSV file by searching the raw data file for missed peaks. Finally, peak pairs were reconstructed, and their chromatographic peak ratios were determined using IsoMS-Quant.

2.3 Statistical analysis

Data cleaning was performed on the provided intensity ratio data. Only those peak-pair features shared by more than 50% of the samples were retained for statistical analysis. Sample imputation was performed on those remaining features missing < 50% data by k-nearest neighbors algorithm using the "Impute" package of the BioConductor package (www.Bioconductor.org) under R (https://cran.r-project.org/). All data was mean-centered and auto-scaled (unit variance) prior to analysis. Multivariate statistical analysis including principal component analysis (PCA), partial least squares discriminant analysis (PLS-DA) along with associated permutation testing was carried out using Metaboanalyst 4.(Xia et al. 2012).VIP values used in part to choose metabolites were calculated by PLS-DA using SIMCA-P + 14.1 (Umetrics, Umeå, Sweden). To calculate *p* value, Student's t-tests were performed using SPSS 25.0 (IBM Corp., Armonk, NY, USA). To estimate the false discovery rate, the multiple-testing-corrected p value (q value) was calculated using R (https

://cran.r-project.org/) and BioConductor(Gentleman et al. 2004) with the package "q value".(Bass JD 2015; Storey 2003) For comparisons between two groups, the area under the curve (AUC), was calculated using Metaboanalyst 4.

Strict selection criteria were then applied to the analyzed data. These criteria were: fold change > 1.5, q value < 0.05, VIP > 1. Only those metabolites meeting these criteria were selected as potential biomarkers.

3 Results

3.1 Study cohort

In total, 27 age and gender-matched samples were added to the cohort for a sum of 50. Batch effects were considered significant, however, and these samples were excluded, leaving a study cohort of 46 MG, 23 RA and 49 controls. Table 1 summarizes patient data.

3.2 Preprocessing

The UMS (universal metabolome-standard method) LC-MS technique, provided broad coverage of both the carboxyl and

Table 1 Demographic data and clinical profiles

Feature	Value
MG	n = 46
Gender (M/F, %)	61/39
Age (years)	59 ± 3.1 (range 19–93)
BMI	28.08 ± 0.56 (range 19.06–34.97)
Class (ocular/generalized, %)	24/76
MMT	4 ± 0.75 (range 0–23)
Age of onset (years)	52 ± 3.3 (range 15–86)
Duration since diagnosis (years)	7 ± 1.1 (range 0–46)
Myasthenia Gravis Medications	(n/46, %)
Pyridostigmine	35 (76)
Prednisone	19 (41)
Azathioprine	14 (30)
Mycophenolate mofetil	7 (15)
Tacrolimus	1 (2)
RA	n = 23
Gender (M/F, %))	71/29
Age (years)	56 ± 3.2 (range 24–84)
RF (% positive)	61.3
BMI	26.18 ± 0.83 (range 19.63–42.57)
Symptom duration (years)	35 ± 4.05 (range 1–75)
Diagnosis duration (years)	37 ± 4.02 (range 1–76)
DAS	4 ± 0.33 (range 1–8)
HAQ	1 ± 0.18 (range 0–4)
ESR	24.54 ± 5.02 (range 0–108)
CRP	13.62 ± 3.91 (range 0.2–86)
Controls	n = 49
Gender (M/F, %)	53/47
Age (years)	49 ± 2.7 (range 19–88)
BMI	27.47 ± 0.55 (range 18.07–36.58)

BMI Body Mass index, *MMT* manual muscle testing, *RF* Rheumatoid factor, *DAS* Disease activity score, *HAQ* Health assessment questionnaire, *ESR* Erythrocyte sedimentation rate, *CRP* C-Reactive protein

phenol/amine serum submetabolomes for all three patient groups: MG, RA and HC. In total, the application of two labelling techniques revealed an overall total of 9954 $^{12}C/^{13}C$ carboxyl-labelled peak pairs (features) and 7458 phenol or amine features after removal of peak-pair features shared by less than 50% of the samples and imputation of those remaining.

3.3 Multivariate modelling

As an initial data survey, principal component analysis was conducted on the different combinations of samples using all peak-pair features.

To further illustrate class separation, initial multivariate modelling of all three groups was performed using principal component analysis (PCA) (supplementary Figure S1) and partial least squares-discriminant analysis (PLS-DA) (supplementary figures S3 and S4).

The acid-labelled groups exhibited excellent discrimination of the three cohorts. The dansyl-labelled groups, while still good, showed less tight clustering and greater overlap of the MG and control groups for the PLS-DA model than the acid-labelled groups, indicating reduced intergroup variability for these samples. MG vs. HC modelling (Figs. 1, 2 and S2) revealed a significant difference between the healthy controls and the MG patients, illustrating good class difference. This group separation was further validated by permutation testing. For all groups the permutation p-value was < 0.05 except for the PLS-DA model of the dansyl-labelled MG-Control groups, at $p = 0.344$. Further, R2cum and Q2cum values were greater than 0.8 for all PLS-DA models, except for the dansyl-labelled MG-Control groups, which expressed limited, but useful predictability at Q2cum = 0.637 (Fig. 1).

3.4 Metabolite identification

After data processing and application of selection criteria, metabolites were matched to in-house standard libraries. A total of 160 individual metabolites were positively identified. Of these, 13 were matched to MG, while 147 were matched to RA. For the remaining features, an accurate mass search of the Human Metabolome Database was undertaken, using the MycompoundID library (Huan et al. 2015). A mass tolerance of 0.005 Da was set as a tolerance cutoff. This search revealed a further 401 putatively-matched metabolites, 19 for MG and 382 for RA. In total, 496 metabolites were either library-matched or putatively identified. Of note also, many metabolites contained carboxyl groups, as a majority of identified metabolites were acid-labelled. Further, benzenoids were heavily represented for both the library-matched and putative metabolites, with six present for each. This was followed by amino acids at five for putatively-matched compounds. Further details on the features of the MycompoundID libraries can be found within the Supplementary Note N1, "Description of the MycompoundID metabolite libraries".

3.5 Discriminating metabolites

Employing the strategy endorsed by Lindahl et al. (Lindahl et al. 2016), criteria-screened metabolites shared by MG and RA were identified and removed from the analysis identifying those unique to MG. After sorting by disease, a total of five library-matched metabolites were identified as unique to MG, and eight metabolites common to both MG and RA.

Of the putatively identified metabolites, seven were unique to MG and 12 common to both groups. No dansyl-labelled metabolites were matched, either by standard library, or putatively, with MG exclusively. Two dansyl-labelled metabolites were identified in *both* the MG and RA samples: Alanyl-Leucine, through the standard libraries and 3-Methoxytyramine, putatively identified by M/Z match.

Of the 5 library-matched metabolites unique to MG, two were short-chain keto acids, two were hydroxy acids, and one was a benzenoid. *Of the 7 putatively identified metabolites unique to MG*, structural lipids dominated with five, accompanied by one organooxygen compound and one bile acid.The total number of metabolites discovered is illustrated by Fig. 3, and further detailed by the Venn diagrams and tables found in supplemental Figs. S5–7 and Tables S6–8. Supplementary Table S9 summarizes the chemical taxonomies and associated pathways for all identified common and unique metabolites, while S10 details the biological roles of each.

3.6 Receiver operating characteristic curves

Metaboanalyst 4.0 was used to generate receiver operating characteristic (ROC) curves for differentiating MG and RA from healthy controls both for individual labelling strategies and combined. Classification models were built using the random forest method based on the five most predictive metabolites as presented in Tables 2 and 3. Biomarker panels were composed of the four library-matched candidate biomarkers and the 5 candidate biomarkers with highest AUC overall. Terephthalic acid was excluded as a xenometabolite, and, therefore, of little predictive value.

As illustrated in Figs. 4 and 5, significant discrimination was evident in both combinations. To obviate any suggestion of overfitting, permutation tests of each ROC curve were undertaken. Using these permutation tests, we did not find any overfitting of the ROC results.

Finally, to evaluate within-model prediction power, a cross-validation was performed for each of the diagnosis panels. Samples were randomly picked and labelled as "new data".

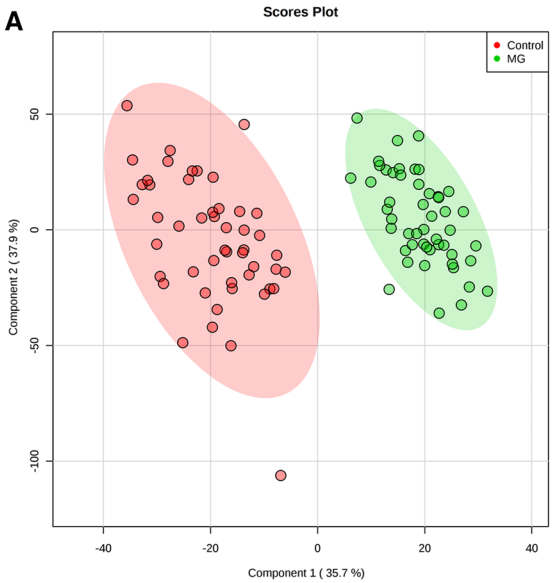

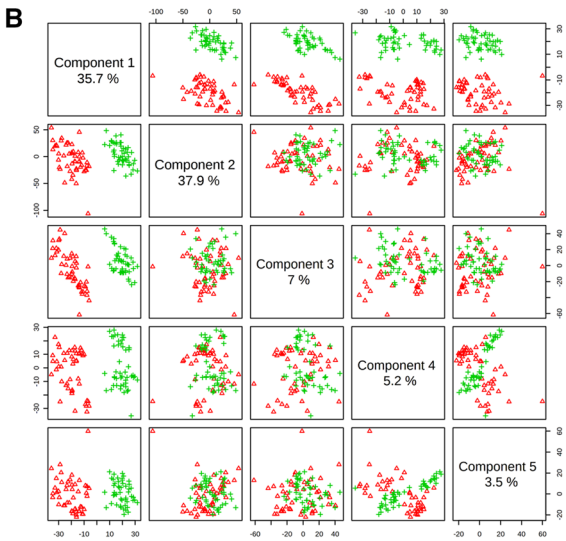

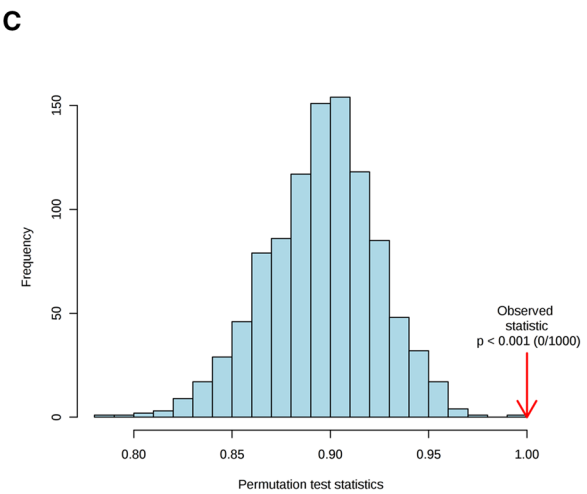

D

Measure	1 comps	2 comps	3 comps	4 comps	5 comps
Accuracy	0.98667	0.99	1	1	1
R2	0.88526	0.92051	0.98184	0.99148	0.99665
Q2	0.8126	0.87167	0.92773	0.94605	0.94727

Fig. 1 Two-dimensional PLS-DA model of acid-labelled MG-Control samples. **a** The PLS-DA model of the MG and Control groups. All observed MS peaks are included in the model; Clear separation of the groups is observed, showing distinct class membership. **b** In total, 89.3% of the total variance was explained by five components with the first three explaining 80.60% of the variance. Further, **c** Cross validation of the PLS-DA showed very good statistical significance with a permutation p-value of < 0.001. **d** 5-component cross validation measures of R2Xcum of 0.997 and Q2cum of 0.947 were also excellent, showing good fit to the data and high predictive ability

Using metaboanalyst, these data were then input into the ROC models of each panel, and the results observed. If the output group information of these samples matches the true group information, the diagnosis model is considered validated by this small internal set of samples. As presented in supplemental Figures, all results showed good predictive power.

4 Discussion

No biomarkers exist that reliably predict the clinical course or therapeutic response in MG. Present biomarkers are primarily diagnostic in nature; both Acetylcholine

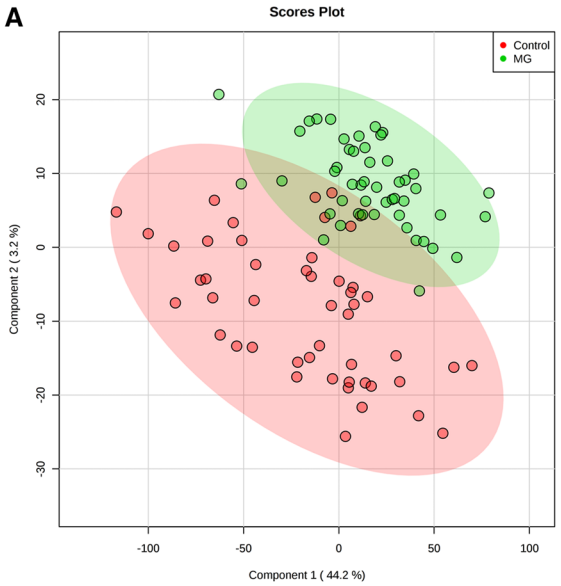

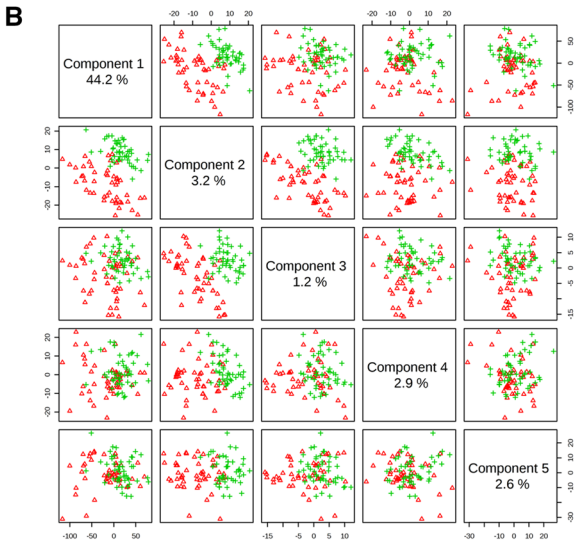

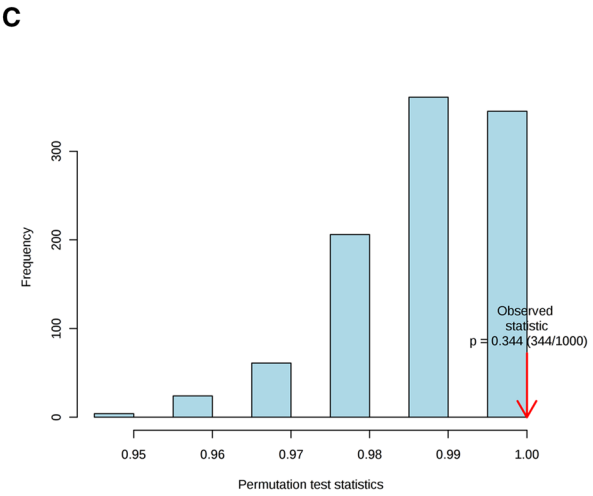

D

Measure	1 comps	2 comps	3 comps	4 comps	5 comps
Accuracy	0.68667	0.83667	0.83667	0.86667	0.88667
R2	0.22512	0.68816	0.87518	0.95488	0.97351
Q2	0.1658	0.51715	0.5367	0.60809	0.63723

Fig. 2 Two-dimensional PLS-DA model of dansyl-labelled MG-Control samples. **a** The PLS-DA model of the MG and Control groups. All observed MS peaks are included in the model; Modest separation of the groups is observed, showing tight class membership. **b** In total, 54.1% of the total variance was explained by five components with the first explaining 44.2% of the variance. Further, **c** Cross validation of the PLS-DA showed somewhat unsatisfactory statistical significance with a permutation p-value of 0.344. **d** 5-component cross validation measures of R2Xcum of 0.973 and Q2cum of 0.637 show good fit to the data, but lower predictive ability than the acid PLS-DA model

receptor (AChR) and anti-MuSK antibodies confirm the diagnosis of MG, but do not correlate with disease severity and/or clinical response (Guptill and Sanders 2010; Howard et al. 1987; Meriggioli and Sanders 2012). Two recent reviews summarize the current state of biomarkers for MG, identifying the need for metabolomic markers (Benatar et al. 2012; Kaminski et al. 2012). Previously, only two studies have explored the metabolomic basis of MG (Lu et al. 2012; Sengupta et al. 2014); a clear need exists for further exploration of metabolomic analysis for the study of MG. In this study we explored the utility of metabolomics to identify metabolites differentially regulated in MG patients compared to healthy volunteers and patients with RA.

We first explored the relationships between the MG, RA and HC cohorts using multivariate analysis. PCA and PLS-DA modelling were used to reveal patterns of between-class variance for both all classes and class pairs for each acid- and dansyl- chemical-labelling strategy. Clear separation was observed for all groups. This is consistent with previous work which not only distinguished MG from healthy controls, (Lu et al. 2012) but also acted as a surrogate measure

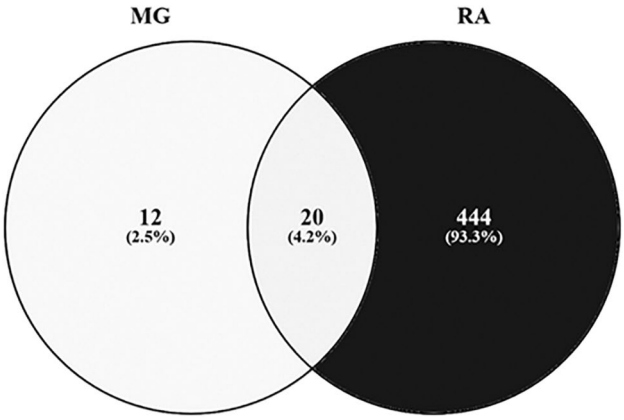

Fig. 3 Venn chart illustrating numbers of significant metabolites identified by group

of disease severity in MG (Sengupta et al. 2014); less severe MG patients were metabolomically distinct from the more severe. Within-class spread was also observed within our MG groups. This may reflect the presence of patients exhibiting significant refractory disease, or duration of disease, possibly representing metabolomically separate subgroups of AChR seropositive MG.

Next, we further investigated the potential of metabolic profiling as a diagnostic tool. Sera from MG and RA patients were observed to have overlapping metabolomic profiles when compared to healthy individuals. The 20 metabolites common to MG and RA were removed from the MG profile on the assumption that these did not represent compounds unique to MG, but rather to more generalized physiological states common to both diseases (such as inflammation). Analysis of these common compounds will be the topic of a parallel manuscript as we seek a better understanding of metabolic profile overlap in antibody-mediated disease. Filtering of common metabolites revealed a set of 12 unique metabolites specific to MG. We found a markedly different metabolic profile in MG patients vs. HC as compared to RA patients vs. HC: 6 metabolites were significantly up-regulated and 6 down-regulated in MG compared to the controls according to stringent AUC, p-values, q-values, VIP and fold-change criteria (Supplementary Table S1.8). Furthermore, the ROC curve analysis of multiple metabolite panels of MG reflected the excellent performance of the applied PLS-DA modelling of metabolic profiles for the discrimination between studied diseases and controls, with cross-validated predictive scores > 80%.

Since our study was focused on AChR seropositive MG, we placed the observed metabolic profile differentiating MG from HC within a biochemical context. Previous work by Lu et al. illustrated significant changes in amino acid, fatty acid, bile acid, structural lipid and oxidative phosphorylation pathways (Lu et al. 2012). Of these, only bile acid metabolism change was observed in our study. Bile acid metabolites were previously observed to be largely downregulated compared to healthy subjects. This was also confirmed by our study, where 12-Ketodeoxycholic acid was likewise observed to be downregulated. Along with their role in the

Table 2 Library-matched metabolites

HMDB	Name	Sample mz	Monoistopic mz	RT	AUC	q-value	VIP	Ratio	FC
HMDB00008	2-Hydroxybutyric acid	104.0472	104.0468	577.24	0.80	3.53E−08	1.78	2.08	2.08
HMDB00011	(R)-3-Hydroxybutyric acid	104.0464	104.0468	610.10	0.83	3.82E−08	0.58	1.60	1.60
HMDB00060	Acetoacetic acid	102.0299	102.0311	913.06	0.81	6.54E−07	2.43	1.75	1.75
HMDB00005	2-Ketobutyric acid	102.0299	102.0311	913.06	0.81	6.54E−07	2.43	1.75	1.75

A total of four metabolites were library-matched and identified as exclusive to the MG group. Library matches were identified using universal metabolite standard method-derived carboxyl and phenol/amine metabolite libraries (MycompoundID)

[a]Terephthalic acid excluded as a xenometabolite

Table 3 Highest AUC metabolites

HMDB	Name	Sample mz	Monoistopic mz	RT	AUC	q-value	VIP	Ratio	FC
HMDB11489	LysoPE(0:0/20:5(5Z,8Z,11Z,14Z,17Z))	499.268	499.2699	1227.72	0.88	3.46E−09	2.27	0.42	−2.36
HMDB00328	12-Ketodeoxycholic acid	390.2757	390.277	2300.92	0.87	2.54E−08	3.15	0.45	−2.24
HMDB11496	LysoPE(0:0/22:6(4Z,7Z,10Z,13Z,16Z,19Z))	525.2857	525.2855	1132.3	0.85	4.67E−07	2.41	0.57	−1.76
HMDB11494	LysoPE(0:0/22:5(4Z,7Z,10Z,13Z,16Z))	527.2992	527.3012	1398.73	0.84	1.11E−07	2.32	0.56	−1.79
HMDB00139	Glyceric acid	106.0253	106.0266	645.02	0.83	1.51E−07	2.12	2.07	2.07

Of those metabolites exclusive to the MG group, five were chosen as potential biomarker candidates based on ROC modelling. Metabolites were either putatively or library-matched with all possessing the highest five AUC values measured

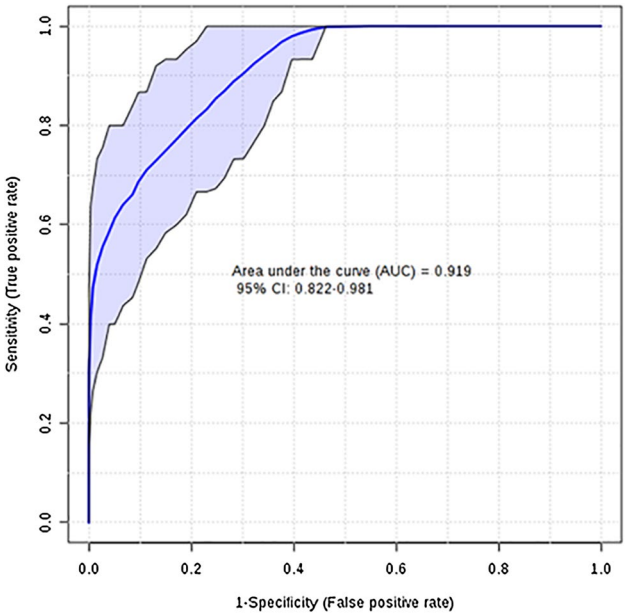

Fig. 4 ROC curve plot for the top four library-matched MG vs. C metabolites panel. ROC curve was created using the random forest algorithm. A total of four metabolites were library-matched and identified as exclusive to the MG group. These metabolites were then input into the model. The model was found to be highly predictive, with an AUC of 0.919

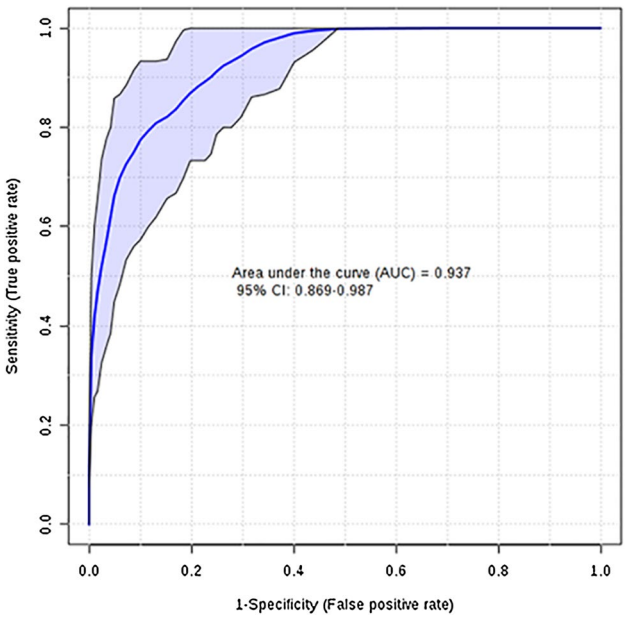

Fig. 5 ROC curve plot for the top highest AUC MG vs. C metabolites panel. ROC curve was created using the random forest algorithm. Of those metabolites exclusive to the MG group, five were chosen as potential biomarker candidates based on ROC modelling. Metabolites were either putatively or library-matched with all possessing the highest five AUC values measured. These metabolites were then input into the model. The model was found to be highly predictive, with an AUC of 0.937

absorption, transport, and metabolism of dietary fats and lipid-soluble vitamins, bile acids have also been implicated in cell signalling, glucose metabolism (Nguyen and Bouscarel 2008) and inflammation (Zhu et al. 2016.). The reason for the observed reduction of bile acids in the MG group remains unclear. Pharmacological effects seem unlikely since while pyridostigmine is subject to metabolism during the first passage through the liver, its hepatotoxicity is quite low. It has been suggested that gut microbiota may reduce the production of bile acids while increasing inflammation, (Staley et al. 2017) although the broader implications for autoimmune disease are uncertain.

Several membrane glycerophospholipids (lysophospholipids) were also changed when compared to controls. This reflects the findings of an earlier paper that also observed perturbation of glycerophospholipid metabolism in response to prednisone treatment in MG patients (Sengupta et al. 2014). Paradoxically, however, where it was previously observed that glycerophospholipids were upregulated in those patients taking prednisone, in our cohort glycerophospholipid downregulation was noted for all patients, including those on prednisone (n = 19, fold-change mean = − 2.71). Pathway-associated glycerolipids (Monoradylglycerolipids) were also found to be downregulated, with MG(0:0/22:5(4Z,7Z,10Z,13Z,16Z)/0:0) exhibiting similar negative fold change to measured glycerophospholipids. Arachidonic acid can be released from activated inflammatory cell membrane phospholipids by phospholipase D (PLA2) (Astudillo et al. 2012; Lone and Taskén 2013). This downregulation of lipids may reflect a higher activity of phospholipase A2 (PLA2), a family of enzymes present in the arachidonic acid pathway, which hydrolyze membrane glycerophospholipids to lysoPCs and fatty acids (Cummings et al. 2000).

A majority of identified metabolites have significant roles within energy production pathways. Glyceric acid is a natural three-carbon sugar acid obtained from the oxidation of glycerol. Several phosphate derivatives of glyceric acid, including 2-phosphoglyceric acid, 3-phosphoglyceric acid, 2,3-bisphosphoglyceric acid, and 1,3-bisphosphoglyceric acid, are important biochemical intermediates in glycolysis (Pollard et al. 2016). Many cells use aerobic glycolysis during rapid proliferation, suggesting an essential role in supporting cell growth. Activated B- and T-cells also experience increases in aerobic glycolysis and oxygen consumption (Boothby and Rickert 2017; Loftus and Finlay 2016; Lunt and Vander Heiden 2011).

In our cohort, upregulation of short-chain keto acids in MG patients compared to controls was observed. This could suggest increased activity in any of several metabolic pathways. 2-ketobutyric acid (a-Ketobutyrate) is involved in the synthesis of aspartic acid, glutamic acid, asparagine, glutamine, ornithine and proline. α-Ketobutyric acid is a

product of the lysis of cystathionine. A byproduct of the lysis of cystathionine, α-Ketobutyric acid is also a degradation product of threonine, resulting from the catabolism of α-Ketobutyric acid by threonine dehydratase. Additionally, 2-ketobutyric acid is produced by the degradation of homocysteine and the metabolism of methionine. α-Ketobutyric acid is also a participant in the citric acid cycle; it is converted into propionyl-CoA Within the mitochondria, then further into methylmalonyl CoA, the finally into succinyl CoA, a citric acid cycle intermediate. Ketone bodies (acetoacetic acid, and β-hydroxybutyric acid) are produced mainly in the mitochondrial matrix of liver cells, from acetyl-CoA when a scarcity of carbohydrates requires that energy must be obtained from the breaking down of fatty acids, in a process called ketogenesis. Ketone bodies are transported from the liver to other tissues, where acetoacetate and β-hydroxybutyrate can be reconverted to acetyl-CoA to produce energy. Some of the acetyl-CoA produced by fatty acid oxidation in liver mitochondria is converted to acetone, acetoacetate and β-hydroxybutyrate. β-hydroxy butyrate ((R)-3-Hydroxybutyric acid) is further converted to acetoacetate for energy. Both are elevated in uncontrolled diabetes mellitus (DMII); due to an absence of insulin, cells, metabolically starved, turn to gluconeogenesis and fat/protein catabolism for energy.

Upregulation of ketone bodies (3-OH-butyrate and acetoacetate) has been also observed in the blood of patients with MS (Cocco et al. 2016). Suggestive of an "energy shift", in conditions of low glucose or carbohydrate concentrations, ketone bodies are produced in mitochondria through fatty acid catabolism. Acetoacetic acid and β-hydroxybutyric acid cross the blood–brain barrier and can be used by cells as an energy source (i.e., converted to acetyl coenzyme A to participate in the citric acid cycle in mitochondria). Impaired glycolysis leading to reduced ATP synthesis may ultimately lead to cell death or degeneration, especially as the mitochondria generates most of the energy for neuronal cells (Lin and Beal 2006).

2-Hydroxybutyric acid (or α-Hydroxybutyrate) may be an early marker of DMII.(Ferrannini et al. 2013;Cobb et al. 2016) Previous work has indicated that high levels of 2-hydroxybutyrate may be an early marker for impaired glucose regulation (Gall et al. 2010a, b). The mechanisms responsible are two-fold: (i) increased lipid oxidation (reflected in an elevated NADH/NAD + ratio) and (ii) oxidative stress. Increases in the production of oxidizing species promote the production of 2-hydroxybutyrate from glutathione metabolism and catabolism of threonine and methionine.(Gall et al. 2010a, b). Further, accumulating evidence has shown that oxidative stress contributes toward the pathogenesis in MG (Adamczyk-Sowa et al. 2017), neurodegenerative disease (Stuerenburg 2000), and inflammatory/autoimmune-mediated tissue damage (Park et al. 2012). Several studies have suggested the relationship between 2-hydroxybutyrate and disorders such as dihydrolipoyl dehydrogenase (E3) deficiency (Tomiko et al. 1983) and cerebral lactic acidosis (Hoffmann et al. 1993). Oxidative stress has also been implicated in the pathogenesis of MS (Lassmann et al. 2012).

Finally, phthalates are xenoestrogenic compounds, environmental toxicants that mimic or induce endogenous hormones. Also known as endocrine disrupting chemicals (EDCs), these include terephthalic acid, which was found to be upregulated in MG. EDCSs can disrupt the immune-neuroendocrine network (INEN), the network joining the endocrine, immune and nervous systems (Manley et al. 2018). Environmental stressors such as phthalate chemical exposure may result in cytokine-induced neurotoxicity by inducing oxidative stress (Franken et al. 2017), and neuroinflammation (Win-Shwe et al. 2013; Yegambaram et al. 2015). Phthalates are also widely used as excipients for the enteric coating of pharmaceutical tablets (Narang and Boddu 2015). Increased terephthalic acid levels may also reflect high-frequency medication schedules, or the taking of large quantities of phthalate-coated medication contiguous with study blood sample collection.

There are multiple drawbacks in our study, which may affect our results. Use of acetylcholinesterase inhibitor and immunosuppressive in the MG patients can change the metabolic profile by introducing new metabolites, and possibly disrupting important immunopathogenic pathways. Larger studies with subgroup analysis is needed to discern the effect of medications. Our patients did not fast prior to sample collection, which can potentially introduce variability in the serum metabolome. Ideally, this would add some measure of consistency, but the nature of opportunist sampling of a rare disease precluded the inclusion of this criteria as logistically unwieldy. In counterpoint, it might be argued that fasting is not consistent with how a metabolomics biomarker would be most useful in clinical practice. In a real-world setting, patients are unlikely to arrive fasting when they present for service. A biomarker panel which retains robust diagnostic reliabilityunder these conditions would be ideal.

5 Conclusion

This study successfully illustrated the potential of LC–MS-based serum metabolomics for rapid identification and distinguishing of MG sera from healthy subjects and a reference autoimmune disease. Metabolomics can play an important diagnostic and prognostic role in clinical medicine, although further work with larger samples remains to correlate the results of previous studies, and possibly those of other autoimmune diseases, to establish robust metabolomic models of MG.

Author contributions DB developed the concept and designed the experiment, acquired all blood samples but those from rheumatoid arthritis patients, conducted all databasing, bioinformatics analyses and metabolite-database matching. Further, DB prepared all charts, images and tables and wrote the paper. ZS provided project oversight as the clinical expert in myasthenia gravis. ZS also offered conceptual advice, supervised project analysis and edited the manuscript. LL developed the chemical labelling process and several chemometric analysis tools used in this study as well as the chemical identification libraries used in the positive identification of observed metabolites. LL provided oversight in the choice of chemical and statistical techniques used to characterize the metabolome. LL also offered conceptual advice, supervised project analysis and edited the manuscript. NW performed the sample preparation, chemical labelling and mass spectrometric analysis. WM provided the rheumatoid arthritis samples for the disease control cohort. All authors reviewed the manuscript.

Compliance with ethical standards

Conflict of interest The authors declare that they have no conflict of interests.

Human research This work received ethics approval from the University of Alberta Research Ethics Board and is in compliance with the ethical standards of this institutional research committee and with the 1964 Helsinki declaration and its later amendments or comparable ethical standards.

Informed consent Informed consent was obtained from all individual participants included in the study.

References

Adamczyk-Sowa, M., Bieszczad-Bedrejczuk, E., Galiniak, S., Rozmiłowska, I., Czyżewski, D., Bartosz, G., et al. (2017). Oxidative modifications of blood serum proteins in myasthenia gravis. *Journal of Neuroimmunology, 305,* 145–153. https://doi.org/10.1016/j.jneuroim.2017.01.019.

Astudillo, A. M., Balgoma, D., Balboa, M. A., & Balsinde, J. (2012). Dynamics of arachidonic acid mobilization by inflammatory cells. *Biochimica et Biophysica Acta (BBA) - Molecular and Cell Biology of Lipids, 1821*(2), 249–256. https://doi.org/10.1016/j.bbalip.2011.11.006.

Bass JD, D. A., & R. D. (2015). qvalue: Q-value estimation for false discovery rate control. *R package version 2.10.0*. http://github.com/jdstorey/qvalue

Benatar, M., Sanders, D. B., Burns, T. M., Cutter, G. R., Guptill, J. T., Baggi, F., et al. (2012). Recommendations for myasthenia gravis clinical trials. *Muscle and Nerve, 45*(6), 909–917. https://doi.org/10.1002/mus.23330.

Boothby, M., & Rickert, R. C. (2017). Metabolic regulation of the immune humoral response. *Immunity, 46*(5), 743–755. https://doi.org/10.1016/j.immuni.2017.04.009.

Cobb, J., Eckhart, A., Motsinger-Reif, A., Carr, B., Groop, L., & Ferrannini, E. (2016). α-hydroxybutyric acid is a selective metabolite biomarker of impaired glucose tolerance. *Diabetes Care, 39*(6), 988–995. https://doi.org/10.2337/dc15-2752.

Cocco, E., Murgia, F., Lorefice, L., Barberini, L., Poddighe, S., Frau, J., et al. (2016). (1)H-NMR analysis provides a metabolomic profile of patients with multiple sclerosis. *Neurology(R) Neuroimmunology & Neuroinflammation, 3*(1), e185. https://doi.org/10.1212/nxi.0000000000000185.

Cummings, B. S., McHowat, J., & Schnellmann, R. G. (2000). Phospholipase A2s in Cell Injury and Death. *Journal of Pharmacology and Experimental Therapeutics, 294*(3), 793–799.

Ferrannini, E., Natali, A., Camastra, S., Nannipieri, M., Mari, A., Adam, K.-P., et al. (2013). Early metabolic markers of the development of dysglycemia and type 2 diabetes and their physiological significance. *Diabetes, 62*(5), 1730–1737. https://doi.org/10.2337/db12-0707.

Franken, C., Lambrechts, N., Govarts, E., Koppen, G., Den Hond, E., Ooms, D., et al. (2017). Phthalate-induced oxidative stress and association with asthma-related airway inflammation in adolescents. *International Journal of Hygiene and Environmental Health, 220*(2), 468–477. https://doi.org/10.1016/J.IJHEH.2017.01.006.

Gall, W. E., Beebe, K., Lawton, K. A., Adam, K.-P., Mitchell, M. W., Nakhle, P. J., et al. (2010a). α-hydroxybutyrate is an early biomarker of insulin resistance and glucose intolerance in a nondiabetic population. *PLoS ONE, 5*(5), e10883. https://doi.org/10.1371/journal.pone.0010883.

Gall, W. E., Beebe, K., Lawton, K. A., Adam, K. P., Mitchell, M. W., Nakhle, P. J., et al. (2010b). α-hydroxybutyrate is an early biomarker of insulin resistance and glucose intolerance in a nondiabetic population. *PLoS ONE, 5*(5), e10883. https://doi.org/10.1371/journal.pone.0010883.

Gentleman, R. C., Carey, V. J., Bates, D. M., Bolstad, B., Dettling, M., Dudoit, S., et al. (2004). Bioconductor: Open software development for computational biology and bioinformatics. *Genome Biology, 5*(10), R80. https://doi.org/10.1186/gb-2004-5-10-r80.

Guptill, J. T., & Sanders, D. B. (2010). Update on muscle-specific tyrosine kinase antibody positive myasthenia gravis. *Current Opinion in Neurology, 23*(5), 530–535. https://doi.org/10.1097/WCO.0b013e32833c0982.

Hoffmann, G. F., Meier-Augenstein, W., Stöckler, S., Surtees, R., Rating, D., & Nyhan, W. L. (1993). Physiology and pathophysiology of organic acids in cerebrospinal fluid. *Journal of Inherited Metabolic Disease, 16*(4), 648–669. https://doi.org/10.1007/BF00711898.

Howard, F. M., Lennon, V. A., Finley, J., Matsumoto, J., & Elveback, L. R. (1987). Clinical correlations of antibodies that bind, block, or modulate human acetylcholine receptors in myasthenia gravis. *Annals of the New York Academy of Sciences, 505,* 526–538.

Huan, T., Tang, C., Li, R., Shi, Y., Lin, G., & Li, L. (2015). MyCompoundID MS/MS search: Metabolite identification using a library of predicted fragment-ion-spectra of 383,830 possible human metabolites. *Analytical Chemistry, 87*(20), 10619–10626. https://doi.org/10.1021/acs.analchem.5b03126.

Hutchinson, D. (1999). Classification criteria: The 1987 American Rheumatism Association revised criteria for the classification of rheumatoid arthritis. *CPD Rheumatology, 1*(1), 13–14.

Kaminski, H. J., Kusner, L. L., Wolfe, G. I., Aban, I., Minisman, G., Conwit, R., et al. (2012). Biomarker development for myasthenia gravis. *Annals of the New York Academy of Sciences, 1275*(1), 101–106. https://doi.org/10.1111/j.1749-6632.2012.06787.x.

Lassmann, H., Van Horssen, J., & Mahad, D. (2012). Progressive multiple sclerosis: Pathology and pathogenesis. *Nature Reviews Neurology, 8*(11), 647–656. https://doi.org/10.1038/nrneurol.2012.168.

Lin, M. T., & Beal, M. F. (2006). Mitochondrial dysfunction and oxidative stress in neurodegenerative diseases. *Nature, 443*(7113), 787–795. https://doi.org/10.1038/nature05292.

Lindahl, A., Forshed, J., & Nordström, A. (2016). Overlap in serum metabolic profiles between non-related diseases: Implications for LC-MS metabolomics biomarker discovery. *Biochemical and Biophysical Research Communications, 478*(3), 1472–1477. https://doi.org/10.1016/J.BBRC.2016.08.155.

Loftus, R. M., & Finlay, D. K. (2016). Immunometabolism: Cellular metabolism turns immune regulator. *The Journal of biological chemistry, 291*(1), 1–10. https://doi.org/10.1074/jbc.R115.693903.

Lone, A. M., & Taskén, K. (2013). Proinflammatory and immunoregulatory roles of eicosanoids in T cells. *Frontiers in Immunology, 4,* 130. https://doi.org/10.3389/fimmu.2013.00130.

Lu, Y., Wang, C., Chen, Z., Zhao, H., Chen, J., Liu, X., et al. (2012). Serum metabolomics for the diagnosis and classification of myasthenia gravis. *Metabolomics, 8*(4), 704–713. https://doi.org/10.1007/s11306-011-0364-6.

Lunt, S. Y., & Vander Heiden, M. G. (2011). Aerobic glycolysis: Meeting the metabolic requirements of cell proliferation. *Annual Review of Cell and Developmental Biology, 27*(1), 441–464. https://doi.org/10.1146/annurev-cellbio-092910-154237.

Manley, K., Han, W., Zelin, G., & Lawrence, D. A. (2018). Crosstalk between the immune, endocrine, and nervous systems in immunotoxicology. *Current Opinion in Toxicology, 10,* 37–45. https://doi.org/10.1016/J.COTOX.2017.12.003.

Meriggioli, M. N., & Sanders, D. B. (2012). Muscle autoantibodies in myasthenia gravis: Beyond diagnosis? *Expert review of clinical immunology, 8*(5), 427–438. https://doi.org/10.1586/eci.12.34.

Narang, A. S., & Boddu, S. H. S. (Eds.). (2015). *Excipient applications in formulation design and drug delivery*. Cham: Springer. https://doi.org/10.1007/978-3-319-20206-8

Nguyen, A., & Bouscarel, B. (2008). Bile acids and signal transduction: Role in glucose homeostasis. *Cellular Signalling, 20*(12), 2180–2197. https://doi.org/10.1016/J.CELLSIG.2008.06.014.

Park, H., Bourla, A. B., Kastner, D. L., Colbert, R. A., & Siegel, R. M. (2012). Lighting the fires within: The cell biology of autoinflammatory diseases. *Nature Reviews Immunology, 12*(8), 570–580. https://doi.org/10.1038/nri3261.

Pollard, T. D., Thomas, D., Earnshaw, W. C., Lippincott-Schwartz, J., & Johnson, G. T. (2016). *Cell biology* (3rd ed.). Amsterdam: Elsevier.

Sengupta, M., Cheema, A., Kaminski, H. J., Kusner, L. L., Gribbestad, I., et al. (2014). serum metabolomic response of myasthenia gravis patients to chronic prednisone treatment. *PLoS ONE, 9*(7), e102635. https://doi.org/10.1371/journal.pone.0102635.

Staley, C., Weingarden, A. R., Khoruts, A., & Sadowsky, M. J. (2017). Interaction of gut microbiota with bile acid metabolism and its influence on disease states. *Applied Microbiology and Biotechnology, 101*(1), 47–64. https://doi.org/10.1007/s00253-016-8006-6.

Storey, J. D. (2003). The positive false discovery rate: A Bayesian interpretation and the q-value. *The Annals of Statistics, 31*(6), 2013–2035. https://doi.org/10.1214/aos/1074290335.

Stuerenburg, H. J. (2000). The roles of carnosine in aging of skeletal muscle and in neuromuscular diseases. *Biochemistry (Moscow), 65*(7), 862–865.

Tomiko, K., Toshihiro, S., Yoshito, I., Masahiro, M., Makoto, Y., Yusuke, S., et al. (1983). Studies of urinary organic acid profiles of a patient with dihydrolipoyl dehydrogenase deficiency. *Clinica Chimica Acta, 133*(2), 133–140. https://doi.org/10.1016/0009-8981(83)90398-4.

Win-Shwe, T.-T., Yanagisawa, R., Koike, E., Nitta, H., & Takano, H. (2013). Expression levels of neuroimmune biomarkers in hypothalamus of allergic mice after phthalate exposure. *Journal of Applied Toxicology, 33*(10), 1070–1078. https://doi.org/10.1002/jat.2835.

Xia, J., Mandal, R., Sinelnikov, I. V., Broadhurst, D., & Wishart, D. S. (2012). MetaboAnalyst 2.0–a comprehensive server for metabolomic data analysis. *Nucleic Acids Research, 40*(W1), W127–W133. https://doi.org/10.1093/nar/gks374.

Yegambaram, M., Manivannan, B., Beach, T. G., & Halden, R. U. (2015). Role of environmental contaminants in the etiology of Alzheimer's disease: A review. *Current Alzheimer Research, 12*(2), 116–146. https://doi.org/10.2174/1567205012666150204121719.

Zhao, S., Luo, X., & Li, L. (2016). Chemical isotope labeling LC-MS for high coverage and quantitative profiling of the hydroxyl submetabolome in metabolomics. *Analytical Chemistry, 88*(21), 10617–10623. https://doi.org/10.1021/acs.analchem.6b02967.

Zhou, R., Tseng, C.-L., Huan, T., & Li, L. (2014). IsoMS: automated processing of LC-MS data generated by a chemical isotope labeling metabolomics platform. *Analytical Chemistry, 86*(10), 4675–4679. https://doi.org/10.1021/ac5009089.

Zhu, C., Fuchs, C. D., Halilbasic, E., & Trauner, M. (2016). Bile acids in regulation of inflammation and immunity: Friend or foe? *Clinical and Experimental Rheumatology, 34*(4 Suppl 98), 25–31.